CI&CEQ
Chemical Industry & Chemical Engineering Quarterly

Available online at
Association of the Chemical Engineers of Serbia AChE
www.ache.org.rs/CICEQ

Chem. Ind. Chem. Eng. Q. 30 (4) 349–357 (2024) CI&CEQ

ITUMELENG KOHITLHETSE
SUTER KIPLAGAT EVANS
MUSAMBA BANZA
ROBERT MAKOMERE

Department of Chemical and Metallurgical Engineering, Vaal University of Technology, Private Bag X021, South Africa

BLAST FURNACE SLAG FOR SO_2 CAPTURE: OPTIMIZATION AND PREDICTION USING RESPONSE SURFACE METHODOLOGY AND ARTIFICIAL NEURAL NETWORK

Article Highlights

- Blast furnace slag preparation and characterization for SO_2 capture
- BFS optimization through Central Composite Design
- Levenberg-Marquardt algorithm in ANN for predicting the performance of the sorbent
- The combined optimization and prediction approach for optimum performance

Abstract

The main reaction parameters examined were the amount of blast furnace slag, the hydration duration, ammonium acetate concentration, and temperature. The Response surface methodology was employed to quantify their impact on the sorbent's surface area. Using a central composite design, the surface area of the resulting sorbent corresponding to Brunauer-Emmett-Teller (BET) was investigated. The sorbents produced range in surface area from 49.89 to 155.33 m^2/g. Additionally, the effectiveness and response prediction capacities of the Response Surface Methodology (RSM) and Artificial Neural Network (ANN) modeling methodologies were investigated. The models were assessed using various statistical metrics, including (MSE) mean squared error, (ARE) average relative errors, the (SSE) sum of squared errors, (HYBRID) Hybrid fractional error function, (SAE) Sum of the absolute errors, (R^2)coefficient of determination, and Root means square. According to statistical evidence, the ANN approach surpassed the RSM-CCD model approach. The surface area of the sorbent was shown to be significantly influenced by interactions between variables in addition to all the individual variables examined. The sorbent was made from a material with substantial structural porosity based on SEM. The functional groups were identified using FTIR. The XRF determined the elemental composition of BFS-based sorbents.

Keywords: blast furnace slag, optimization, central composite design, artificial neural network, response surface methodology.

SCIENTIFIC PAPER

UDC 669:66:621:519.87

The control of atmospheric pollution brought on by combustion processes like coal has recently been subject to stricter environmental restrictions worldwide.

Correspondence: I. Kohitlhetse, Vaal University of Technology, Departement of Chemical and Metallurgical Engineering, Bag X021, Vanderbijlpark, South Africa.
E-mail: 222386568@edu.vut.ac.za
Paper received: 17 July, 2023
Paper revised: 5 February, 2024
Paper accepted: 4 March, 2024

https://doi.org/10.2298/CICEQ230717006K

The most plentiful and cost-effective energy source is coal, essential for supplying the world's rising need for electricity [1]. Burning coal provides various difficulties even if it is a significant energy source. The discharge of pollutants, particularly sulphur dioxide, into the environment is one of the most critical problems facing enterprises that burn coal. Sulphur in coal combines with air during combustion to create sulphur dioxide (SO_2). Sulphur dioxide is one of the many contaminants in our atmosphere (SO_2) [2]. Burning things containing sulfur releases a harmful gas into the atmosphere. All types of coal and oil include sulphur. Industrial facilities that use fossil fuels to produce energy or extract metal

from ore are the primary sources of SO_2 emissions (smelter). Other anthropogenic sources include locomotives, ships, and other large vehicles or equipment that burn sulphur-rich fuel. Volcanoes are the sole crucial natural source of SO_2. Only roughly one-third of all SO_2 emissions into the atmosphere come from volcanoes. Volcanic SO_2 has little effect in South Africa because no active volcanoes exist [3].

Both direct SO_2 exposure and secondary pollutants created when SO_2 combines with other airborne molecules negatively affect health. A significant secondary contaminant associated with SO_2 is delicate particulate matter. Exposure to SO_2 results in immediate symptoms such as breathing difficulties, respiratory system injury, and a burning sensation in the nose, throat, and lungs. Severe and long-term health effects include early death, heart and lung disease, dementia, and problems with conception [4]. They also have diminished cognitive function. Aside from the harmful effects on human health, every combustion process that releases SO_2 releases large volumes of greenhouse gases into the environment. SO2 sources thus have a disadvantageous immediate consequence on the region's health and a negative long-term impact on human well-being globally due to greenhouse gas emissions, which drive global warming.

Several SO_2 emission control techniques based on emission prevention or flue gas capture turned out to be investigated, and some came to be implemented in sulphur dioxide-discharging industries. Since sulphur dioxide emissions are proportional to the amount of sulphur in fuel and the total used in combustion, reducing sulphur content can result in significant reductions. Using ultra-low sulphur flue is the most environmentally friendly way to reduce sulphur dioxide emissions; however, obtaining cleaner flue comes at a high refining cost [4]. Installing a sulphur restoration unit that generates profit-making sulphur in the form of sulphuric acid is an option if the gas flow consists of a high concentration of sulphur and the restoration unit can withstand the corrosive environment associated with acid sulphur [5]. In industries that use coal as a fuel source, sulphur in pyrite (Fe_2S) can be easily removed by physically washing coal with water. However, increased practical costs and fuel-efficient design property changes could offset this. Even though many treatment methods, including WFGD (FGD), biological processes, and technological innovations based on electron beam irradiation, can achieve high sulphur removal efficiency, several problems still need to be solved, including high space requirements and high safety protection requirements [6]. Coronal pulse discharge, on the other hand, is a relatively new and unproven SO_2 removal method, even though it does not require a particle accelerator and offers the highest level of protection. Because of its simplicity and high desulphurization capacity, flue gas desulphurization (FGD) is the most frequently used method to reduce SO_2 emissions [7].

A variety of sorbents that are various chemical compounds and naturally occurring materials can be quickly produced, or waste generated by a variety of processes can be used in the method. Several flue gas desulphurization (FGD) techniques are water- self-sufficient, resulting in lower operating costs and no wastewater production. It is necessary to utilize the proper Flue Gas Desulphurization (FGD) technology to reduce SO2 emissions into the environment [8]. Coal combustion produces coal fly ash, another type of combustion waste, and pollutants like sulphur dioxide (SO2). Researchers have looked into flue gas desulphurization using absorbent synthesis from a combination of calcium hydroxide, calcium oxide, and calcium sulphate to address these difficulties [9]. Numerous studies have shown that, for instance, when coupled with Ca (OH)2 or CaO during the hydration process, coal ash can create an absorbent with a higher SO2 capture capacity than hydrate lime [2,8,10].

Blast Furnace Slag (BFS), a byproduct of the iron and steel industry, has promise as a practical and affordable substitute sorbent for flue gas desulphurization technology. The two main ingredients for removing SO_2 are abundant in BFS: CaO and silica. They produce Calcium Silicate Hydrate Aggregates, which are essential for increasing the surface area of the Sorbent. According to some studies, sorbent made of iron blast furnace slag and hydrated lime (BFS/HL) exhibits higher SO_2 reactivity than hydrated lime alone under the dry or semi-dry FGD method [4]. It is clear from earlier sources that the production of high surface area calcium silicate hydrates during the sorbent preparation or slurring process is caused by an enhancement in the sorbent's reactivity patterns, using calcium, or the capacity to capture SO_2 [4].

When a dependent output variable is impacted by several independent input factors rather than one factor at a time, the response surface methodology is a statistical method for optimizing the process [11]. The output variable's name is the response. RSM assesses all process factors concurrently while predicting an outcome as an improved systematic approach to experimentation. The central composite design is one of the critical components of RSM. The experiments used a three-level experimental design called the central composite design, which combined the axial and factorial design points. Its key benefit is that it demands multiple experimental runs to determine the

proper conditions for experimentation [12].

A model of computation called an artificial neural network can be used to predict how biological neurons process input. Most neural network models feature hidden layers in addition to input and output layers; the number depends on the inquiry type of investigation [8]. The primary property of a neural network is its ability to carry out internal calculations to derive the desired output from a set of input data. Given enough data, the ANN can evaluate multifactorial, non-linear, linear, and complex procedures by training the multiple input-output networks technique [13,14]. Because it reliably and effectively depicts the non-linear interactions between the variables and responses of various processes, ANN may be used in intricate systems [15].

In the current study, the surface area was assessed by BET analysis by investigating the effect of BFS amount, the ammonium acetate amount, hydration time, and hydration temperature. With the fewest experiments, the RSM approach enables the study of the individual variables and their combined impacts in the experimental range. This study's main objective is to evaluate the surface area of BFS for SO_2 capture using RSM and ANNs, estimate their effectiveness, and compare ANN and RSM techniques. The experimental data was then compared to the outcomes of the two models.

MATERIALS AND METODS

Raw materials

The Blast furnace slag was collected from a local company around Vanderbijlpark, South Africa. The ammonium acetate (>98%) and the calcium oxide (>97%) were all purchased from Merck, and the brine sludge was collected from a local chloral alkali industry.

Sorbent preparation of the sorbent

A known quantity (250 g) of brine sludge was heated for 4 hours, and 900 °C was set as the temperature in a furnace with muffles for maximal calcination. 200 mL of distilled water was heated to 65 °C, and 10 g of CaO was added while vigorously agitated. A certain amount (0–1 g) of ammonium acetate as the hydration agent and blast furnace slag (0–5 g) were added to the slurry at the same time. The hydration process was then accelerated by heating the blast furnace slag slurry for a set amount of time (1–10 hours) at a certain hydration temperature (30–90 °C). The resulting slurry underwent filtration for 2 hours at 210 °C during drying. The powdered sorbents were pelletized, smashed, and crushed to less than 75 μm to produce the required nanoparticle size.

Characterization of the sorbent

The functional compounds contained in the sorbent were examined using Fourier transform infrared spectroscopy (PerkinElmer UATR). Scanning electron microscopy (Philips XL30FEG) was employed to assess the shape of the surface. X-ray fluorescence (Philips expert 0993) was used for qualitative as well as quantitative techniques. The materials' BET surface area and pore volume were measured using an N2 sorption-desorption apparatus and ASAP 2020 Micromeritics.

Analysis using artificial neural networks and the response surface approach

Centrale composite design in Response surface methodology

Recent years have seen a rise in interest in response surface methodology (RSM), a set of mathematical and statistical methods for assessing the effects of numerous independent variables. RSM assesses the relationships between the response(s) and the independent variables, in addition to the effects of individual variables on the processes, whether operating alone or in conjunction [11]. This approach provides many benefits, including being less costly, requiring fewer experiments, exploring how different factors interact to affect response, predicting a response, assessing method suitability, and consuming less time [16]. This strategy employs low-order polynomial equations in a predefined area of the independent variables to attempt to find the optimal values for the independent variables for the most positive results. The sorbents' BET surface area was investigated using the CCD. This design helps assess how the sorbent preparation variables affect the sorbent's particular surface area. The variables for sorbent preparation explored are hydration time, BFS amount, hydrating agent (ammonium acetate) amount, and hydration temperature. The RSM analysis consists of 21 experimental data sets, with six central points.

According to Eq. (1), the response was calculated using an empirical second-order polynomial equation.

$$z = X0 + XaA + XbB + XcC + XdD + XaaA^2 + XbbB^2 + XccC^2 + XddD^2 + XabAB + XacAC + XadAD + XbcBC + XbdBD + XcdCD \quad (1)$$

where Z is the predicted outcome; X_0 denotes the model constant; Xa, Xb, Xc, and d denote linear coefficients; Xab, Xac, Xad, Xbd, and Xcd denote cross-product coefficients, and Xaa, Xbb, Xcc, and Xdd denote quadratic coefficients. A, B, C, and D denote independent variables.

The experimental design, analysis of variance, regression analysis, and optimization of process parameters in the desulphurization process were carried out using Design-Expert 13. ANOVA p-value and the regression coefficient (R^2) were used to assess the model's acceptability.

The steps in the optimization process are as follows: choosing the process variables and responses; choosing the experimental design; conducting experiments to gather data; fitting the model equation to the experimental data; performing an analysis of variance (ANOVA); and finally, determining the optimal conditions [17].

Artificial neural network (Levenberg-Marquardt)

Three-layer system: one neuron on the output layer, one hidden layer with six different modes, four neurons on the input layer, and measurements of hydration temperature, BFS, and ammonium acetate (4-6-1). The most common network, known as a back-propagation (BP-ANN) network, trains an approach for modeling data from experiments using a first-order gradient descent technique. It works well to cut down on errors with each repeat. Out of various back-propagation (BP) methods, we chose the Marquardt-Levenberg learning strategy. In the simulation and prediction of the sorbent production using ANN, the log-sigmoid function of transfer (log sig) in the layer that was hidden with four neurons in the first layer and a linear transfer function in the output node were both used. Modular artificial neural networks were developed using the Neural Networks (NN) toolbox and the mathematical application MATLAB 2022a. The ANN model's configuration processes involve the following steps: collecting data, training and test set selection, conversion of data into ANN inputs, identifying, training, and testing network structures, if necessary, repeating the processes several times to get the best model, and implementation of the best ANN model [13].

Error analysis functions

The Root mean square error (RMSE), Mean square errors (MSE), Average relative errors (ARE), Hybrid fractional error function (HYBRID), Sum of squares of errors (SSE), and Sum of absolute errors (SAE) Statistical evaluation tests were used to prove that the models were satisfactory [16]. The non-linear methods presented in Eqs. (2–7) were used to compare data from experiments with model-predicted data.

$$RMSE = \sqrt{\frac{1}{N}\sum_{i=1}^{n}\left(\frac{\left(Z_{(e)}-Z_{(p)}\right)^2}{Z_{(e)}}\right)} \quad (2)$$

$$SSE = \sum_{i=1}^{n}\left(Z_{(e)}-q_{(p)}\right)^2 \quad (3)$$

$$SAE = \sum_{i=1}^{n}\left[\left(Z_{(e)}-Z_{(p)}\right)\right] \quad (4)$$

$$HYBRID = \frac{1}{N-M}\sum_{i=1}^{n}\left(\frac{\left(Z_{(e)}-Z_{(p)}\right)^2}{q_{e(e)}}\right)x100 \quad (5)$$

$$ARE = \frac{100}{M}\sum_{i=1}^{n}\left(\left[\frac{\left(Z_{(e)}-Z_{(p)}\right)^i}{Z_{(e)}}\right]\right) \quad (6)$$

$$MSE = \frac{1}{N}\sum_{i=1}^{n}\left(Z_{(e)}-Z_{(p)}\right)^2 \quad (7)$$

where N is the total number of measurements, M is the maximum amount of model parameters, and $Z(p)$ and $Z(e)$ are the expected and measured values, expressed as m^2/g, respectively.

RESULTS AND DISCUSSION

The morphological analysis

Figure 1a depicts the morphological appearance of the blast furnace using SEM. An irregularly shaped structure of various sizes with a smooth surface was readily seen in the sample. The increased magnification shows the high structural porosity of the particle. Figure 1b shows SEM micrographs of sorbents after treatment. Before sulphation, the sorbent's overall pore structure and irregularly shaped particle arrangement are seen in the image. The sorbent has open spaces, implying that sulphation reactions can occur [8].

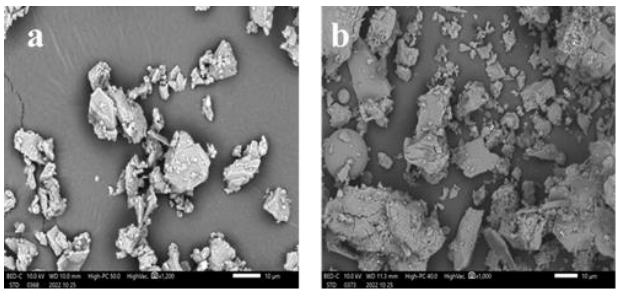

Figure 1. SEM of (a) the blast furnace and (b) after treatment.

Fourier-transform infrared spectroscopy Analysis

Figure 2 shows the antisymmetric vibration of the Ca-O and Si-O-Si bonds due to the strong, intense peak between 570 and 1100 cm^{-1} in the raw blast furnace slag. Because of the presence of calcium

hydroxide, the hydroxyl group is thought to be stretching vibrational bonds around 3500 cm^{-1}, which is related to the weak absorption band. In all the figures, the absorption peak associated with the C-O vibrations in the carbonate structure can be seen at 1600 cm-1 and roughly 700 cm^{-1}. The Ca-O vibration bond is attributed to the significant absorption band at 587 cm^{-1}. Silica and calcium oxide, which are essential in expanding the surface area of the sorbents, are among the components that make up the functional group present [4].

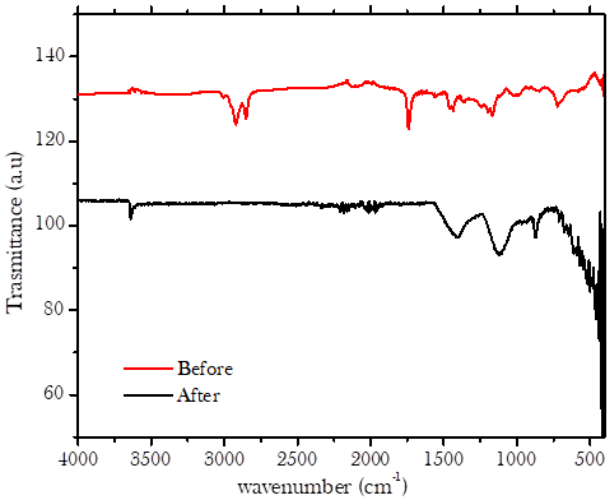

Figure 2. FTIR of the blast furnace slag.

X-Ray Fluorescence analysis

Table 1 below provides the chemical breakdown of BFS before and after treatment as determined by XRF analysis. The total element found in blast furnace slag makes up most of the complex heterogeneous substance known as BFS. After treatment, some elements are absent in the sorbent due to the sulphation and calcination process reaction.

Table 1. The elemental composition of the sorbent.

		Before treatment		After treatment	
Element	Line	Mass %	Atom %	Mass %	Atom %
C	K	7.78	24.63	23.32	39.59
O	K	5.09	11.99	33.23	42.19
Mg	K	0.52	0.8	1.11	0.92
Si	K	1.72	2.32		
S	K	14.36	16.91		
Ca	K	4.11	3.88	34.13	17.3
Mn	K	47.42	32.58		
Fe	K	8.85	5.95		
Au	M	11.69	2.24	9.5	0.98

Response surface plots

A CCD was used to assess the impact of four experimental factors on the area region of an absorbing material made from blast furnace slag. The resulting sorbent's surface area corresponding to Brunauer-Emmett-Teller (BET) was investigated. The sorbents produced range in surface area from 49.89 to 155.33 m^2/g. The surface area of the sorbent is a function of hydration temperature and ammonium acetate content. Figure 3a illustrates the variations in absorbing material surface dimensions as a function of the ammonium acetate concentration (B) and hydration temperature (D). The sorbent surface area significantly increases when large volumes of ammonium acetate are employed. The production of Very significant hydroxyl complexes having a wide area of contact is facilitated by hydrating agents, which may be the cause for this. Although high temperatures raise the sorbent's surface area, when the reaction time is lengthened, the sorbent's surface area also grows over time [18]. The pozzolanic reaction has been reported to create calcium silicate-hydrated compounds at higher temperatures and longer hydration times [19]. Figure 3b shows how the sorbent surface area changes; it expands when the ammonium acetate level is significant. This demonstrates unequivocally that the moisturizing agent ammonium acetate enhances the hydration level of a hydroxide aggregate with a large surface area. The surface area of the sorbent also increases with the addition of more blast furnace slag. The phenomenon is explained by the fact that when more bagasse is used, calcium oxide and more silica are combined, producing more calcium silicate [20].

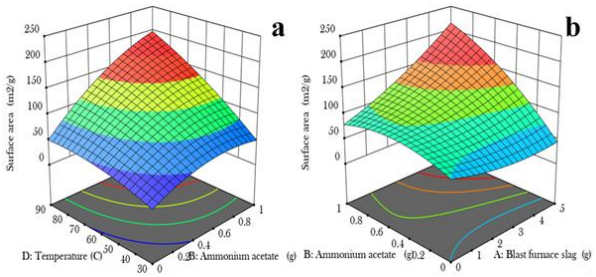

Figure 3. The interaction between (a) temperature and ammonium acetate and (b) blast furnace slag and ammonium acetate on the surface area.

Eq. (8) is produced by the final model displayed below after Fisher's Test is used to exclude the irrelevant terms.

$$Surface\ area = +110.42 + 27.69A + 44.89B - 7.98C + 45.13D + 40.48AB - 3.43AC + 28.96AD + 0.4900BC + 28.91BD - 10.29CD + 12.21A^2 - 20.57B^2 + 15.11C^2 - 11.31D^2 \quad (8)$$

By contrasting the factor coefficients, the coded equation can be used to determine the relative importance of the elements. A positive sign in front of the phrases indicates a synergistic influence, whereas an antagonistic influence is shown by a negative sign [11]. The results of these statistical tests indicate that the regression model equations properly show the link

between the important experimental parameters and the surface area of the sorbent. It is evident through regression analysis that the coefficient for hydration temperature (D) is the largest of all the variables. Therefore, we can conclude that this variable significantly impacts the surface area of sorbents made from blast furnace slag.

The analysis of variance (ANOVA) was used to confirm that the model was adequate by testing for variance-based variations in means between two or more category groups; an ANOVA test is a sort of statistical test used to assess if there is a statistically significant difference variable. Table 3 displays this at a 95% confidence level. The third-order algebraic equation was put to the test. A regularly distributed continuous dependent variable and two or more categorical independent variables (factors) make up a two-way ANOVA (analysis of variance). The model is suggested to be significant by the model's *F*-value of 13.56. An *F*-value this big might happen owing to noise only 0.21% of the time [21].

When the *P*-value is less than 0.0500, model terms are regarded to be significant. A, B, C, D, AB, AD, BD, CD, and B2 are crucial model terms. If the value exceeds 0.1000, model terms are not significant. If your model includes many unnecessary terms (apart from those required to maintain hierarchy), removing them may improve the performance. The lack of fit *F*-value of 45.31 suggests that the lack of fit is considerable. Noise can result in a substantial Lack of Fit F-value only 0.18% of the time. A significant lack of fit in the model is undesirable since we want it to fit. Temperature (D) possessed a major impact on surface area (C) relative to ammonium acetate content (A). In contrast to variables A and B, the quadratic terms D greatly impacted the surface of the absorbent area. The C variable has very minimal influence on the surface region of the sorbent. The absorbing material surface region is unaffected by the cubic expression. The interaction between components B and C does not significantly affect the surface area.

While the other stayed constant, the impact of one factor was assessed and plotted versus surface area. Compared to the other three criteria, hydration substantially affected surface area more. Ammonium acetate concentration came next, and then the impact of time and hydration on blast furnace slag. The surface area rises with temperature and ammonium acetate concentrations. Raising hydration length and hydration time has little effect on surface area [8]. Table 2 also exhibits the impact. A high *F*-value for the hydration temperature indicates that it likely significantly impacts the surface area.

Table 2. ANOVA.

Source	Sum of Squares	df	Mean Square	*F*-value	*p*-value	
Model	15353.31	14	1096.67	13.56	0.0021	significant
A-Blast furnace slag	1532.92	1	1532.92	18.95	0.0048	
B-Ammonium acetate	4029.33	1	4029.33	49.81	0.0004	
C-Time	636.36	1	636.36	7.87	0.0310	
D-Temperature	4073.79	1	4073.79	50.36	0.0004	
AB	2621.42	1	2621.42	32.41	0.0013	
AC	94.12	1	94.12	1.16	0.3222	
AD	1341.89	1	1341.89	16.59	0.0066	
BC	1.92	1	1.92	0.0237	0.8826	
BD	1337.26	1	1337.26	16.53	0.0066	
CD	847.07	1	847.07	10.47	0.0178	
A^2	380.84	1	380.84	4.71	0.0731	
B^2	1079.75	1	1079.75	13.35	0.0107	
C^2	582.46	1	582.46	7.20	0.0364	
D^2	326.49	1	326.49	4.04	0.0913	
Residual	485.35	6	80.89			
Lack of Fit	464.83	2	232.41	45.31	0.0018	significant

R^2 = 0.952; R^2 Predicted = 0.925; R^2 Adjusted = 0. 954.

Artificial Neural network

The backpropagation method of Levenberg-Marquardt was used to train the MLP network (4:6:1). However, it generally takes more Space, so this approach is quicker. This happens when the validation samples' mean square error increases, indicating that generalization is no longer improving. The best number of neurons in the hidden layer, the best number of validation and training data, and the best number of testing samples were all determined using this technique [13]. Of the 21 samples employed in the ANN modeling, 70% (15 samples), 15% (3 samples), and 15% (3 samples) were used for training, testing, and training validation, respectively. The network's interactions with training, testing, and validation data are depicted in Figure 4. Correlation coefficients for training, testing, validation, and total data were determined to be 0.999, 0.994, 0.964, and 0.992, respectively. The straight line also demonstrates a linear relationship. The experimental (goal) and forecasted (output) results are related. The results suggest high agreement between the actual data and

the data predicted by the model. Therefore, the coefficient of total correlation reveals the excellent prediction capacity of the developed ANN model, making it suitable for correctly predicting data [22].

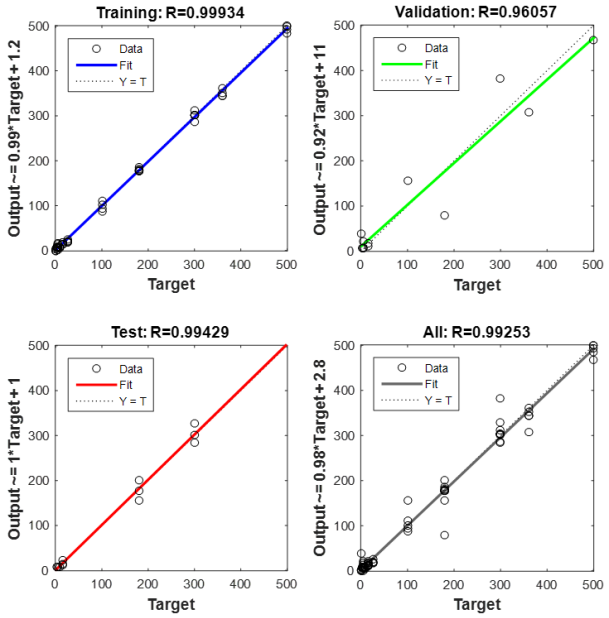

Figure 4. Neural network regression analysis.

Predicted and actual data RSM and ANN

The actual (experimental) and anticipated values for the surface area are compared and statistically analyzed in Table 3. According to the results, both models can adequately predict the surface area. The RMSE, MSE, ARE, HYBRID, SSE, SAE, and R^2 values for the RSM model were all found to be 0.065, 0.049, 0.024, 0.314, 0.018, 0.198 and 0.952, respectively, whereas the ANN model was found to be 0.009, 0.020, 0.012, 0.188, 0.06, 0.110 and 0.992. Both models provide relevant statistical data, according to statistics, indicating that they may be used in this procedure [15]. The accuracy of the RSM and ANN techniques in displaying actual and expected results is seen in Table 3. The linear fit also shows both models' remarkable capabilities. Although both models can predict the surface, the ANN model displayed better RMSE, MSE, ARE, HYBRID, SSE, SAE, and R^2 values.

Both models could accurately predict the sorbent's surface area, the Response surface method, and the Artificial neural network. The artificial neural network (ANN) was implemented in Table 4 to maximize the sorbent's surface area [15].

Table 3. Comparison of artificial neural networks (ANN) and Response surface method (RSM).

Run	Blast furnace slag (g)	Ammonium acetate (g)	Hydration period (hrs)	Hydration temperature (°C)	Surface area(m^2/g) RSM	ANN
1	5	1	8	30	112.71	113.22
2	5	1	2	30	116.62	116.98
3	5	0	8	90	68.6	70.25
4	0	1	2	90	142.18	145.24
5	5	0	2	90	115.64	115.96
6	0	0	8	30	89.18	90.01
7	0	1	8	90	110.74	112.25
8	0	0	2	30	81.34	80.97
9	0	0.5	5	60	99.96	100.00
10	5	0.5	5	60	155.33	156.32
11	2.5	0	5	60	49.96	50.98
12	2.5	1	5	60	139.75	140.21
13	2.5	0.5	2	60	133.18	135.29
14	2.5	0.5	8	60	127.69	130.39
15	2.5	0.5	5	30	58.99	60.28
16	2.5	0.5	5	90	149.25	150.22
17	2.5	0.5	5	60	104,46	105.85
18	2.5	0.5	5	60	101.48	100.40
19	2.5	0.5	5	60	105.17	105.98
20	2.5	0.5	5	60	107.60	108.95
21	2.5	0.5	5	60	103.34	105.37
				RMSE	0.065	0.009
				MSE	0.049	0.020
				ARE	0.024	0.012
				HYBRID	0.314	0.188
				SSE	0.018	0.006
				SAE	0.198	0.110
				R^2	0.952	0.992

Table 4. The optimum predicted conditions.

Variables	Values
Reaction time	5 h
Reaction temperature	60°C
Ammoniumacetate	0.5 g
BFS	5 g
Surface area	150.00 m^2/g

CONCLUSION

This study demonstrated that it is possible to prepare sorbent for DFGD. SEM micrographs indicated high porosity and open spaces, which show that there is room for sulphation reaction. Silica and calcium oxide were identified in the functional group that was observed on the FTIR. The results show that when blast furnace slag is employed as a pozzolan substance, a pozzolanic reaction occurs that results in aggregation of hydrated calcium silicates, expanding the area of the sorbent's surface. RSM analysis revealed that the sorbent preparation variables significantly affect the final sorbent surface area. Higher blast furnace slag and ammonium acetate content increased surface area; a moderate rise was seen at high temperatures and during lengthy hydration time. A quadratic model was developed to link the independent variables and the surface area. The RMSE, MSE, ARE, HYBRID, SSE, SAE, and R^2 values for the RSM model were all found to be 0.065, 0.049, 0.024, 0.314, 0.018, 0.198 and 0.952, respectively, whereas the ANN model generated 0.009, 0.020, 0.012, 0.188, 0.06, 0.110 and 0.992. This can be due to the small number of datasets available for application. Working with a lot of different data sets may be more effective for the ANN model.

ACKNOWLEDGMENTS

The author would like to acknowledge the Department of Chemical and Metallurgical Engineering at Vaal University of Technology for providing continuous operational resources.

ABBREVIATION

ANN	Artificial neural network
BFS	Blast furnace slag
RMSE	Root means square errors
ARE	Average relative errors
MSE	Mean square errors
CCD	Central composite design
BP	Back-propagation
FGD	Flue gas desulphurization
DFGD	Dry flue gas desulphurization
WFGD	Wet flue gas desulphurization
LM	Levenberg-Marquardt model
ML	Multilayer perceptron
HL	Hydrated lime
MPSD	Derivative of Marquardt's percent standard deviation
RMSE	Root means square errors
BP	Back-propagation
LM	Levenberg-Marquardt model

REFERENCES

[1] B.J. Shokri, F. Shafaei, F.D. Ardejani, S. Entezam, Soil Sediment Contam. 32 (2023) 23–40. https://doi.org/10.1080/15320383.2022.2090895.

[2] L. Lerotholi, R.C. Everson, L. Koech, H.W.J.P. Neomagus, H.L. Rutto, D. Branken, B. B. Hattingh, P. Sukdeo, Clean Technol. Environ. Policy 24 (2022) 2011–2060. https://doi.org/10.1007/s10098-022-02308-y.

[3] C. Zheng, K. Li, C. Zhang, D. Deng, Sep. Sci. Technol. 56 (2021) 2499–2506. https://doi.org/10.1080/01496395.2020.1833218.

[4] R.S. Makomere, H.L. Rutto, L. Koech, Arabian J. Sci. Eng. 48 (2022) 8871–8885. https://doi.org/10.1007/s13369-022-07491-0.

[5] A. López-Olvera, S. Pioquinto-García, J. Antonio Zárate, G. Diaz, E. Martínez-Ahumada, J.L. Obeso, V. Martis, D.R. Williams, H.A. Lara-García, C. Leyva, C.V. Soares, G. Maurin, I.A. Ibarra, N.E. Dávila-Guzmán, Fuel 322 (2022) 124213. https://doi.org/10.1016/j.fuel.2022.124213.

[6] X. Li, T. Huhe, T. Zeng, X. Ling, Z. Wang, H. Huang, Y. Chen, Heliyon 8 (2022) 11463. https://doi.org/10.1016/j.heliyon.2022.e11463.

[7] G. Long, C. Yang, X. Yang, T. Zhao, M. Xu, J. Mol. Liq. 302 (2020) 112538. https://doi.org/10.1016/j.molliq.2020.112538.

[8] R. Makomere, H. Rutto, L. Koech, H. Rutto, L. Koech, J. Environ. Sci. Health, Part A 58 (2023) 191–203. https://doi.org/10.1080/10934529.2023.2174334.

[9] D. Gazioglu Ruzgar, S. Altun Kurtoglu, M.F. Fellah, J. Nat. Fibers 19 (2022) 1366–1375. https://doi.org/10.1080/15440478.2020.1764459.

[10] Y. Yu, R. Zhao, J. Chen, H. Yao, Chem. Eng. J. 431 (2022) 134267. https://doi.org/10.1016/j.cej.2021.134267.

[11] M. Banza, H. Rutto, Int. Nano Lett. 12 (2022) 257–272. https://doi.org/10.1007/s40089-022-00369-x.

[12] S. Chellapan, D. Datta, S. Kumar, H. Uslu, Chem. Data Collect. 37 (2022) 100806. https://doi.org/10.1016/j.cdc.2021.100806.

[13] M. Banza, H. Rutto, T. Seodigeng, Soil Sediment Contam. Int. J. 0 (2023) 1–21. https://doi.org/10.1080/15320383.2023.2178384.

[14] C. Mgbemena, S. O. Onyegu, Qeios (2023) 32388. https://doi.org/10.32388/GEGPL7.

[15] A.A. Ayoola, F.K. Hymore, C.A. Omonhinmin, O.C. Olawole, O.S.I. Fayomi, D. Babatunde, O. Fagbiele, Chem. Data Collect. 22 (2019) 100238. https://doi.org/10.1016/j.cdc.2019.100238.

[16] J. Kabuba, M. Banza, Results Eng. 8 (2020) 100189. https://doi.org/10.1016/j.rineng.2020.100189.

[17] M. Banza, H. Rutto, Can. J. Chem. Eng. 101 (2023) 896–908. https://doi.org/10.1002/cjce.24384.

[18] Z. Zhao, K. Patchigolla, Y. Wu, J. Oakey, E.J. Anthony, H. Chen, Fuel Process. Technol. 221 (2021) 106938. https://doi.org/10.1016/j.fuproc.2021.106938.

[19] J.X. Liu, J. Li, W.Q. Tao, Z. Li, Fluid Phase Equilib. 536 (2021) 112963. https://doi.org/10.1016/j.fluid.2021.112963.

[20] J. Lim, J. Kim, Fuel 327 (2022)124986. https://doi.org/10.1016/j.fuel.2022.124986.

[21] J.R. Hanumanthu, G. Ravindiran, R. Subramanian, P. Saravanan, J. Indian Chem. Soc. 98 (2021)100086. https://doi.org/10.1016/j.jics.2021.100086.

[22] D.S.P. Franco, F.A. Duarte, N.P.G. Salau, G.L. Dotto, Chem. Eng. Commun. 206 (2019) 1452–1462. https://doi.org/10.1080/00986445.2019.1566129.

ITUMELENG KOHITLHETSE
SUTER KIPLAGAT EVANS
MUSAMBA BANZA
ROBERT MAKOMERE

Department of Chemical and Metallurgical Engineering, Vaal University of Technology, Private Bag X021, South Africa

NAUČNI RAD

ŠLJAKA VISOKE PEĆI ZA HVATANJE SO_2: OPTIMIZACIJA I PREDVIĐANJE POMOĆU METODOLOGIJE POVRŠINE ODZIVA I VEŠTAČKE NEURONSKE MREŽE

Glavni istraživani reakcioni parametri bili su količina šljake visoke peći, trajanje hidratacije, koncentracija amonijum-acetata i temperatura. Metodologija površine odziva (MPO) u kombinaciji sa centralnim kompozitnim planom je korišćena za kvantifikovanje njihovog uticaj na površinu sorbenta po Brunauer-Emet-Teleru (BET). Površina dobijenhi sorbenata se kreću od 49,89 do 155,33 m^2/g. Pored toga, istražena su efikasnost i kapaciteti predviđanja odgovora metodologija MPO i veštačke neuronske mreže (VNM). Modeli su procenjeni korišćenjem različitih statističkih metrika, uključujući srednju kvadratnu grešku, prosečnu relativnu grešku, (SSE) zbir kvadratnih grešaka, hibridnu funkciju frakcione greške, zbir apsolutnih grešaka, koeficijent determinacije, a koren srednje kvadratne vrednosti. Prema statističkim dokazima, VNM model je nadmašio pristup MPO modela. Pokazalo se da na površinu sorbenta značajno utiču interakcije između faktora pored svih pojedinačnih faktora. Prema SEM-u, sorbent je napravljen od materijala sa značajnom strukturnom poroznošću. Funkcionalne grupe su identifikovane korišćenjem FTIR. Rentgenskm analizom je određen elementarni sastav sorbenata.

Ključne reči: šljaka visoke peći, optimizacija, centralni kompozitni plan, veštačka neuronska mreža, metodologija površine odziva.